Climate Dynamics (2023) 60:2041–2059
https://doi.org/10.1007/s00382-022-06419-6

Assessment of the RegCM4-CORDEX-CORE performance in simulating cyclones affecting the western coast of South America

Natália Machado Crespo[1] · Michelle Simões Reboita[2] · Luiz Felippe Gozzo[3] · Eduardo Marcos de Jesus[1] · José Abraham Torres-Alavez[4,5] · Miguel Ángel Lagos-Zúñiga[6,7,8] · Limbert Torrez-Rodriguez[9] · Marco Reale[4,10] · Rosmeri Porfírio da Rocha[1]

Received: 15 April 2022 / Accepted: 5 July 2022 / Published online: 2 August 2022

Abstract
In this study, we assess the performance of the Regional Climate Model version 4 (RegCM4) in simulating the climatology of the cyclones near the west coast of South America. The synoptic evolution and seasonality of these systems are thoroughly investigated. The analyses are based on four simulations from the CORDEX-CORE Southern America (SA) domain, at 0.25° of horizontal resolution: one driven by ERA-Interim and three driven by different GCMs. The reference dataset is represented by ERA5. Cyclones were detected by an objective scheme in the period 1995–2005 and classified in three different classes: (i) Coastal Lows (CLs) and cyclones affecting the coast (CAC) (ii) crossing and (iii) not crossing the Andes. In general, RegCM4 is able to reproduce the climatology of cyclones affecting the western coast of SA. In particular: (i) CLs are shown to be more frequent in austral summer although their frequency is underestimated by the simulations in this season; (ii) CAC not crossing the Andes represent 76% of all CAC and are more frequent in winter, with simulation underestimating their frequency by ~22% due to the differences in the simulated upper-level jets, which tend to get weaker (by ~5–10 m s^{-1}) northwards of 30°S; (iii) the frequency of CAC crossing the Andes tends to be overestimated mainly in winter, which is associated with the combination of the stronger upper-level jets and weaker SLP in the simulations, especially southwards of 40°S.

Keywords Coastal lows · Western South America · Cyclones · Regional climate modeling · Climatology

1 *Introduction*

Cyclones are an important component of the atmospheric circulation and to the hydrological cycle over Southern America (SA). They are a relevant source of precipitation and also of extreme wind and precipitation events (e.g. Pezza and Simmonds 2005; Reboita et al. 2019; Dalagnol et al. 2022). Many studies have already discussed the climatology and dynamics of cyclones over the eastern part of the continent (Gan and Rao 1991; Seluchi 1995; Vera and Vigliarolo 2000; Pezza and Ambrizzi 2003; Hoskins and Hodges 2005; Reboita et al. 2010, 2012, 2015, 2018, 2020, 2021; Crespo

✉ Natália Machado Crespo
nataliacrespo@alumni.usp.br

1 Instituto de Astronomia, Geofísica e Ciências Atmosféricas, Universidade de São Paulo, São Paulo, SP, Brazil

2 Instituto de Recursos Naturais, Universidade Federal de Itajubá, Itajubá, MG, Brazil

3 Departamento de Física e Meteorologia, Faculdade de Ciências, Universidade Estadual Paulista, Bauru, SP, Brazil

4 Earth System Physics, The Abdus Salam International Centre for Theoretical Physics, Trieste, Italy

5 Institute for Atmospheric and Climate Science, ETH Zürich, Zürich, Switzerland

6 Center for Climate and Resilience Research, Universidad de Chile, Santiago, Chile

7 Advanced Mining Technology Center, Universidad de Chile, Santiago, Chile

8 Civil Engineering Department, Universidad de Chile, Santiago, Chile

9 Universidad de La Serena, La Serena, Chile

10 National Institute of Oceanography and Applied Geophysics-OGS, Trieste, Italy

et al. 2021; de Jesus et al. 2021). On the other hand, fewer works describe the dynamics of these mid-latitudes systems over the western part (Garreaud et al. 2002; Garreaud and Rullant 2004; Rasmussen and Houze Jr 2016; Scaff et al. 2017; Gómez-Contreras et al. 2021). Besides extratropical cyclones (ECs), the climatology of the synoptic systems influencing the weather over the western SA (in ~ 30°S) also includes cyclones known as Coastal Lows (Garreaud et al. 2002; Gómez -Contreras et al. 2021), which are associated with migratory anticyclones and the orographic barrier of the Andes. In addition, subtropical cyclones also occur in southeastern South Pacific (Yanase et al. 2014), however, to the authors' best knowledge, only one case study described the processes conducting to subtropical cyclogenesis in this region (Silva et al. 2022).

As highlighted by several authors (e.g. Barrett et al. 2009; Garreaud 2009; Aceituno et al. 2021), the dynamics of the synoptic disturbances reaching the extratropical Andes is strongly influenced by the presence of mountains. Many of the cyclones move from the central South Pacific and reach the west coast of SA (e.g. Simmonds and Keay 2000; Reboita et al. 2015; Marrafon et al. 2021). Numerous studies (e.g. Reboita et al. 2020; Crespo et al. 2021) show a clear maximum density of cyclones between 40°S and 50°S and extending from 90°W towards the SA west coast. ECs transport humidity eastwards and, in function of the low-level circulation, the air might be forced to ascend when interacting with the Andes, enhancing orographic precipitation events in Central-Southern Chile (Aceituno et al. 2021; Valenzuela and Garreaud 2019; Espinoza et al. 2020).

Many ECs that affect the western SA, southwards of 30°S, are associated with cutoff lows, cold closed lows in the mid-upper levels of the atmosphere detached from the westerlies (Palmen and Newton 1969; Fuenzalida et al. 2005; Reboita et al. 2010; Pinheiro et al. 2017; Muñoz et al. 2020) and potential vorticity cutoffs (Crespo et al. 2021; Portmann et al. 2021). Some of these systems can develop surface cyclogenesis, and they represent an important mechanism for generating precipitation in the coastal western Andes, specifically in the Northern-Central portion of Chile (Fuenzalida et al. 2005; Barahona 2013; Reboita and Veiga 2017; Muñoz and Schultz 2021) around 24°S, where they account for up to 50% of the annual rainfall (Aceituno et al. 2021).

Coastal Low (hereafter CL) was defined by Garreaud et al. (2002) as "shallow warm-core low pressure cells with alongshore and cross-shore scales of 1000 and 500 km, respectively". The genesis of CLs is associated with a migratory surface anticyclone over southern Chile (~ 40°S), which propitiates offshore south-quadrant low-level wind that, in general, are reinforced by the southerly winds of the eastern portion of the South Pacific Subtropical High (SPSH). As the migratory anticyclone moves towards northeast, adiabatic and stretching processes contribute to the CL development as follows: the air from the south part of the anticyclone ascends when approaching the Andes Mountains - being adiabatically cooled - and the air column shrinks, consequently, increasing the anticyclonic rotation (see Fig. 4.11 from Holton and Hakim 2013). At same time, in the north part of the anticyclone the air parcel is heated by adiabatic compression when it blows down from the mountains to the coast, followed by a decrease of the anticyclonic vorticity due to the stretching of the air column, leading to the formation of a CL. The downslope motion is further reinforced by the west side of the trough at mid-upper level associated with the cold air incursions over SA (see Fig. 8 from Garreaud 1999). From the climatological point of view, the eastern side of the SPSH, north of 35°S (25°S) in austral summer (winter), is characterized by a trough at the surface, which is associated with the Andes subsidence (e.g. Rahn and Garreaud 2014; Crespo et al. 2021; Andrelina and Reboita 2021).

CLs are more frequent during the austral winter around 30°S, while in the other seasons the maximum tends to shift towards ~ 34°S (Gómez-Contreras et al. 2021). According to these authors, in ERA5 reanalysis, the seasonal average frequency of CLs is of 7 systems in summer, 8 in autumn, 12 in winter and 12 in spring. Furthermore, CLs cause relevant and different weather changes over the coast and further in the inland areas of Chile. CLs produce offshore flows and enhanced subsidence in the subtropical coast, with a shallow maritime boundary layer, stratocumulus dissipation, and warm conditions. In the northern sector of the CLs, the strengthened westerlies cause cloudy and moist conditions. Moreover, as CLs are associated with the occurrence of enhanced subsidence over the continent (Muñoz et al. 2020), large temperature oscillation, drier and stable conditions, clear skies, high temperatures at ~ 1000 m occur, and therefore a worsening of the air quality in Santiago (Rutllant 1981; Rutllant and Garreaud 1995, 2004; Gallardo et al. 2002; Saide et al. 2011).

Since the CLs and ECs significantly affect the weather on the west coast of SA and there are only few studies analyzing the ability of regional climate models in simulating them (e.g. Garreaud and Rutllant 2003; Reboita et al. 2020, 2021), the aim of this study is to evaluate the performance of the RegCM4 (Giorgi et al. 2012) in simulating these systems over the western coast of SA. The RegCM4 was chosen for its good performance on simulating important climate aspects in the SA domain, especially cyclones (e.g. Reboita et al. 2020; de Jesus et al. 2021).

This paper is structured as follows: Background section, discussing the classes of cyclones that will be addressed in this study; Data and Methods, describing the datasets

used and the methodology applied to identify and sort the cyclones, based on the Background section; Results and Discussion, discussing the climatological features of the cyclones in the simulations compared to ERA5; and a final section of Conclusions.

2 Background

The two types of low-pressure systems affecting the weather of the southwestern coast of SA to the south of 17°S, the ECs and the CLs, present different synoptic patterns, life cycles and impacts on the continent. Thus, this section discusses an example of each type aiming to help readers to follow the results and conclusions (Sects. 4 and 5) more easily.

The synoptic descriptions are based on sea level pressure (SLP), geopotential height at 500 hPa, equivalent potential temperature (θ_e) at 850 hPa, cyclonic relative vorticity (RV) and air temperature at 925 hPa, relative humidity and horizontal wind from 1000 to 400 hPa from the ERA5 reanalysis. Also, 24 h accumulated precipitation from CPTEC-MERGE (Rozante et al. 2010) is used. Synoptic fields are shown at the time when the systems' circulation (cyclonic RV at 925 hPa) reaches the coast.

The ECs are synoptic-scale low pressure systems typically associated with the passage of mid-upper troposphere troughs over a region of strong low-level baroclinicity (Schultz et al. 2019 and references therein) 20212022 They may form near the Chilean coast or farther west (over the South Pacific), later moving eastwards and reaching the continent. In the latter case, ECs may impact Chile already in its mature stage, with well developed fronts. An illustrative example of this kind is an EC that caused widespread precipitation in central-southern Chile on June 30, 2000 (Fig. 1c). Accumulated daily precipitation reached 50 mm near the coast and up to 130 mm in localized areas along the Andes. The cyclogenesis of this EC occurred on June 28, around 110°W, with a pronounced baroclinic trough configured at 500 hPa (figure not shown). When the cyclone reached the continent, on June 30, it was already in its mature stage, with an equivalent barotropic structure (located at 80°W-50°S in Fig. 1a). The associated cold front is evident in Fig. 1b as a region of sharp θ_e gradient and strong cyclonic RV near 34°S. Ahead of this frontal zone, the northeastern flow transports warmer and wetter (higher θ_e) air from lower latitudes towards Chile, configuring an atmospheric river that fuels the precipitation events over central-southern areas of the country. In this example, the EC effectively moved over the South American coast, but sometimes they can influence the coastal weather even when their center stays and decays away from the coast. For this reason, they will be referred to as "cyclones affecting the coast" (CACs).

An example of CL occurred during the first days of July, 2000, just after the EC described before. An area of high pressure with 1016 hPa moved from the west (Fig. 2a), and when it was located beneath the 500 hPa ridge, it strengthened to 1024 hPa and merged with the SPSH (Fig. 2b). Two days later, the elongated anticyclone flow contributed to the formation of the CL (Fig. 2c). This development is in line with the conceptual model of CLs formation presented by Garreaud et al. (2002) and later studies (e.g. GómezContreras et al. 2021). On July 05, the CL is identified by the relatively low pressure near the coast at around 73°W-23°S (Fig. 1d). The zonally elongated SPSH can also be seen in the SLP field, and the geopotential height field displays the 500 hPa ridge, whose axis by this time was over Argentina. This synoptic situation is associated with warming and drying weather in most of Chile - high temperatures reach latitudes up to 40°S (Fig. 1e). The 925 hPa horizontal wind in this figure also shows a cyclonic circulation alongshore from 20°S to 35°S. It can be inferred that central and northern coastal Chile is under the influence of Andes' downslope winds, known in central Chile as Raco Wind (e.g. Muñoz et al. 2020). The effects of CL in weather conditions can be illustrated by the vertical variations of horizontal winds, air temperature and relative humidity over north and central Chile (Fuenzalida et al. 2005; Barahona 2013; Reboita and Veiga 2017; Muñoz and Schultz 2021), and are exemplified for Santiago (70.5°W-33.5°S) in Fig. 1 f.

This section highlights that CAC and CL features, development and coastal impacts are significantly different. However, the automatic tracking method (Sect. 3.2) does not discriminate between them, so cyclones need to be sorted out after the tracking process before further analyses. The sorting method, based on characteristics described in this section, is presented in Sect. 3.3.

3 Data and methods

3.1 RegCM4 simulations and ERA5 reanalysis

The climatologies of cyclones here analyzed are based on a set of four different simulations produced with the Regional Climate Model version 4 (RegCM4, Giorgi et al. 2012) in the context of CORDEX-CORE project (Giorgi et al. 2022): one driven by ERA-Interim (evaluation run, Dee et al. 2011) and three driven by the global climate models (GCMs) from the Coupled Model Intercomparison Project (CMIP5; climate runs; Taylor et al. 2012). The GCMs used are: (i) Hadley Center Global Environment Model version 2 (HadGEM2-ES; Collins et al. 2008), (ii) Max Planck Institute

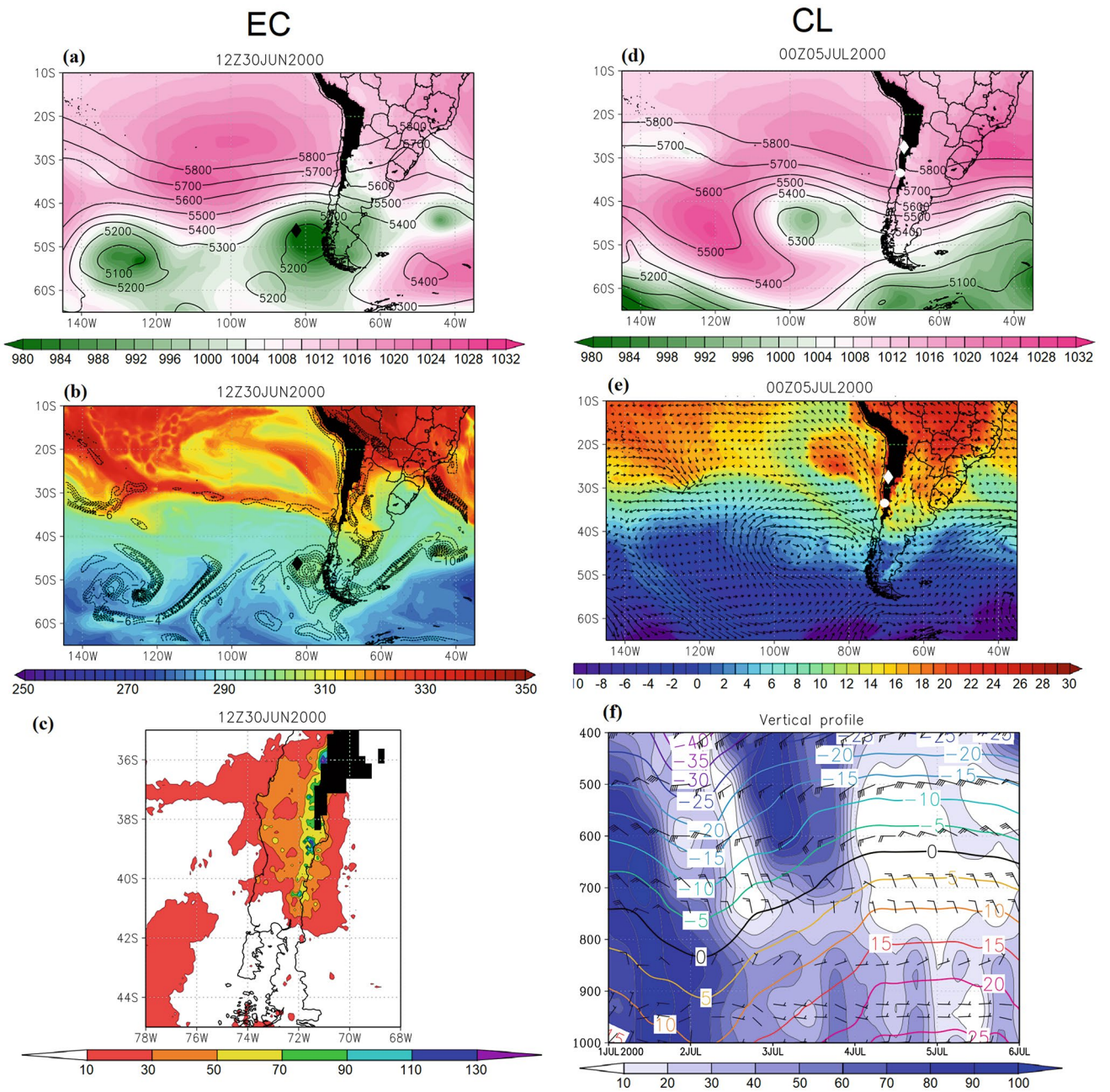

Fig. 1 Synoptic maps from ERA5 reanalysis illustrating the two main types of cyclones that impact Chile. **(a)**, **(d)** 500 hPa geopotential height (black lines, in m) and SLP (shaded, in hPa) for EC and CL, respectively. Black (white) diamonds indicate the EC (CL) position determined by the tracking algorithm; **(b)** EC 850 hPa equivalent potential temperature (shaded, in K) and 925 hPa cyclonic relative vorticity (in 10^{-5} s^{-1}); **(c)** EC accumulated precipitation from CPTEC-MERGE (in mm day^{-1}); **(e)** CL 925 hPa air temperature (shaded, in °C) and winds (vectors, in m s^{-1}); **(f)** vertical profile of temperature (lines, in °C), relative humidity (shaded, in %) and horizontal wind from 0000UTC 01 July 2000 to 0000UTC 06 July 2000 in the city of Santiago [white dots in figures **(d)** and **(e)** indicate the location of Santiago (70.5°W-33.5°S)]

Earth System Model (MPI-ESM-MR; Giorgetta et al. 2013), and (iii) Norwegian Earth System Model (NorESM-1 Bentsen et al. 2013). The choice of these GCMs as drivers to RegCM4 was originally based on their relatively good performance in reproducing the mean climate over the CORDEX-CORE regions (Elguindi et al. 2014) and by the fact that they cover the range of possible climate sensitivities in the CMIP5 ensemble (Teichmann et al. 2021). Once the three GCM-driven simulations have ability in reproducing the features of CL and CAC in the present climate - object of the present work - they could be used in further studies to provide an insight on possible future climate changes

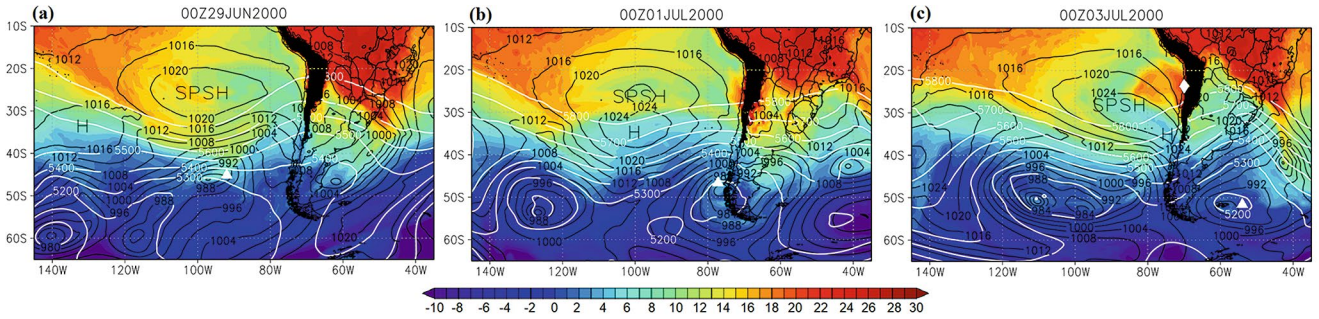

Fig. 2 Synoptic maps from ERA5 reanalysis in the days prior to the formation of the CL. SLP (black contours, in hPa), geopotential height at 500 hPa (white contours, in m) and air temperature at 925 hPa (shaded, in °C) are presented for **(a)** 0000 UTC 29 June, **(b)** 0000 UTC 01 July and **(c)** 0000 UTC 03 July, 2000. SPSH stands for South Pacific Subtropical High and H stands for the transient anticyclone. The white diamond in **(c)** indicates the position of the CL, and the white triangles in **(a-c)** indicate the position of the EC determined by the tracking algorithm.

of these systems. The dynamical downscaling in the four simulations were carried out using 25 km as horizontal grid spacing and 23 sigma-pressure levels.

In the scientific literature, the analysis of the reconstructed EC activity over a specific area suffers from an important limitation. In fact, while for tropical cyclones the observational tracks are usually available, for ECs no reference tracks exist and, thus, it is difficult to assess the reliability of the simulated cyclone activity and of the related weather fields (e.g. wind and precipitation). In general, the approach followed in this case is to compare the simulated cyclone activity with an ensemble of models or with reanalysis, which uses model to assimilate all observational dataset available to reconstruct atmospheric variables, such as ERA-Interim or ERA5, which should provide the best possible estimation of the synoptic field employed to detect and track cyclones.

In this work we use ERA5 as a reference dataset (Hersbach et al. 2020) to evaluate the simulated cyclone activity and associated synoptic atmospheric variables. The reason for such a choice relies on the fact that ERA5 has been shown to exhibit several improvements in the SLP and wind fields with respect to former ERA-Interim (Belmonte Rivas and Stoffelen 2019; Dullaart et al. 2020; Molina et al. 2021), which have been widely used so far as reference data to evaluate cyclone activity and associated synoptic patterns (e.g. Neu et al. 2013; Flaounas et al. 2018; Reboita et al. 2020; 2021) over different CORDEX domains. Moreover, ERA5 has finer resolution than other reanalyses, being more suitable to evaluate local scale processes such as flow-topography interaction, which play a fundamental role in the dynamics of CLs. At the same time, it has a similar resolution to the simulations and this should make the comparison more straightforward (Reale et al. 2021).

The period of evaluation of the RegCM4 performances is 1995–2005 with a specific focus on the extended austral winter and summer seasons: June-July-August-September-October-November (hereafter JJASON/winter) and December-January-February-March-April-May (hereafter DJFMAM/summer) respectively.

3.2 The cyclone tracking algorithm

Over the last decades, different automatic schemes have been adopted to detect and track cyclones. Each of these approaches reflects the lack of consensus on what a cyclone really is, which results, in turn, in the use of different physical variables such as SLP or RV to reconstruct the climatologies of cyclones in a specific area (e.g. see Neu et al. 2013). Several studies based on the IMILAST dataset (e.g. Neu et al. 2013; Ulbrich et al. 2013; Lionello et al. 2016; Flaounas et al. 2018; Reale et al. 2019) have pointed out that the choice of a specific variable to detect and track cyclones could influence the resulting climatology. Because of that, the use of different automatic schemes on the same original dataset should be a better approach for describing the life cycle of cyclones. However, as the purpose of this study is to evaluate the performance of RegCM4 in reproducing the main feature of the cyclones over the west coast of SA, the evaluation of the sensitivity of climatologies to different cyclone definitions is left for a further study.

Cyclones are identified and tracked with an automatic scheme in ERA5 and RegCM4 datasets. The scheme computes the RV by using 6-hourly u and v wind components at 925 hPa and identifies the minima of RV using the nearest-neighbor approach. For each cyclone, the algorithm provides latitude, longitude and the RV at the center. Only cyclones with lifetime ≥ 24 h and initial RV $\leq -1.5 \times 10^{-5}$ s^{-1} are included in the study (for more details see Reboita et al. 2010). The domain chosen for the tracking is 95.0ºW-21.0ºW and 15.0ºS-54.5ºS. Being a limited domain, cyclones can enter in the analysis area or have genesis inside it. Then, we will not focus on the cyclogenesis but in the cyclone stage when they reach the west coast of SA. In the case of CLs, they have their genesis always inside the domain.

3.3 Classification of coastal lows and cyclones reaching the coast

We adopted the following criteria to separate the cyclones detected by our tracking scheme in CL and CAC:

i) First, we select all cyclones whose centers are located westwards of 71°W;
ii) A cyclonic center is classified as CL if its genesis occurs within 71°-76°W and 20°-35°S (their typical region of formation, as exemplified by the case in Sect. 2) and if the distance traveled is ≤ 1500 km (since CLs are considered stationary systems);
iii) Cyclones that are not CLs are considered CAC when they reach the longitudinal band of 71°W-85°W. As shown in Sect. 2, important weather impacts may be occurring along the coast while the cyclone center is tracked far off over the South Pacific (Fig. 1b). This can also happen when the cyclone center is even farther, but their fronts extend toward the coast associated with continental precipitation, for example. The longitudinal band was chosen to account for these two situations;
iv) Finally, we also separate the CACs in those crossing the Andes and those dissipating near the coast. For those crossing Andes, we only considered systems southwards of 40°S when they reach the continent at 71°W.

3.4 Validation of the simulations

The track densities of the simulated systems are compared with those from ERA5. Statistics significance tests for the track densities were not computed since they tend to be very unequal and difficult to analyze (Pezza et al. 2008, 2012).

The same will be done for the synoptic composite fields of CLs and CACs. For the CLs we analyze − 48 and − 24 h apart from their genesis. For the CACs we first consider the timestep when cyclones reach 85°W and then (based on this timestep) we select − 24 and 24 h apart from this timestep for the cyclone's life cycle. It is important to note that the precipitation composite is represented by the accumulated precipitation during the cyclones' life cycle inside the latitudinal range of 85°-71°W for the ones that do not cross the Andes, i.e., when they are expected to affect the coast. The variables used for both cyclones categories are based on case studies (discussed in Sect. 2). In that sense, for CL we analyze SLP, temperature at 925 hPa, and geopotential height at 500 hPa. For CAC we considered the same fields together with specific humidity and horizontal moisture transport at 850 hPa, accumulated precipitation, and upper-level winds at 250 hPa.

4 Results and discussion

This section aims to describe the seasonal climatological aspects of CLs and CACs in terms of genesis and track densities, the large-scale evolution, and to validate the simulations through comparisons. In both cases ERA5 is used as reference.

4.1 Coastal lows (CLs)

Figure 3 presents the seasonal frequency of CLs genesis and track densities. CLs are more frequent during austral summer than in winter. During summer there are two centers of genesis around 30°S, whereas in the winter CLs maxima are more meridionally extended and their offshore displacement is shorter than in summer (Fig. 3a-b). Nevertheless, the track densities show that CLs travel short distances in both seasons (443.5 ± 73.6 km for all cases), in agreement with literature (Garreaud et al. 2002; Garreaud and Rutllant 2003).

Regarding the simulation biases, there is an underestimation of the frequency of CL genesis and track density in summer equatorwards of 35°S, whereas polewards there is an overestimation (Fig. 3c,e,g,i). Biases in the track density are quite similar among the four simulations, although RegNor shows greater underestimation, which might be due the coarser resolution and to a weaker simulated SPSH in the driving GCM (figure not shown), which negatively impacts the frequency of CL formation. In winter the simulations mainly overestimate genesis and track densities of CLs (Fig. 3d,f,h,j), especially RegERAI. One explanation for the overestimation might be due to the more intense simulated SPSH and the tendency of the driving dataset to simulate its location closer to the continent. In addition, the four simulations underestimate the track density around 33°S (especially RegMPI).

Figures 4 and 5 show ERA5 and the simulation biases of the synoptic evolution from 48 h prior until the CLs formation during austral winter. In the 48-hours time window previous the genesis (-48), a trough at 500 hPa with an axis around 80ºW moves towards the South Atlantic (Fig. 4a; the same pattern occurs in austral summer). 24-hours after (-24), the trough practically crosses the Andes (south of 40°S) with a northwest orientation of its axis over the west coast of SA, driving the adiabatic heating of the atmospheric column near the coast of Chile. Near the surface, the SPSH core shows a strengthening and a displacement towards the west coast. As the anticyclone approaches the continent, its southern (northern) sector ascends (descends) the Andes. Then, the adiabatic heating is amplified by the mid-level trough which reduces the sea surface pressure leading to the CL genesis (from − 24 to 0 h; Fig. 4a). This pattern occurs in

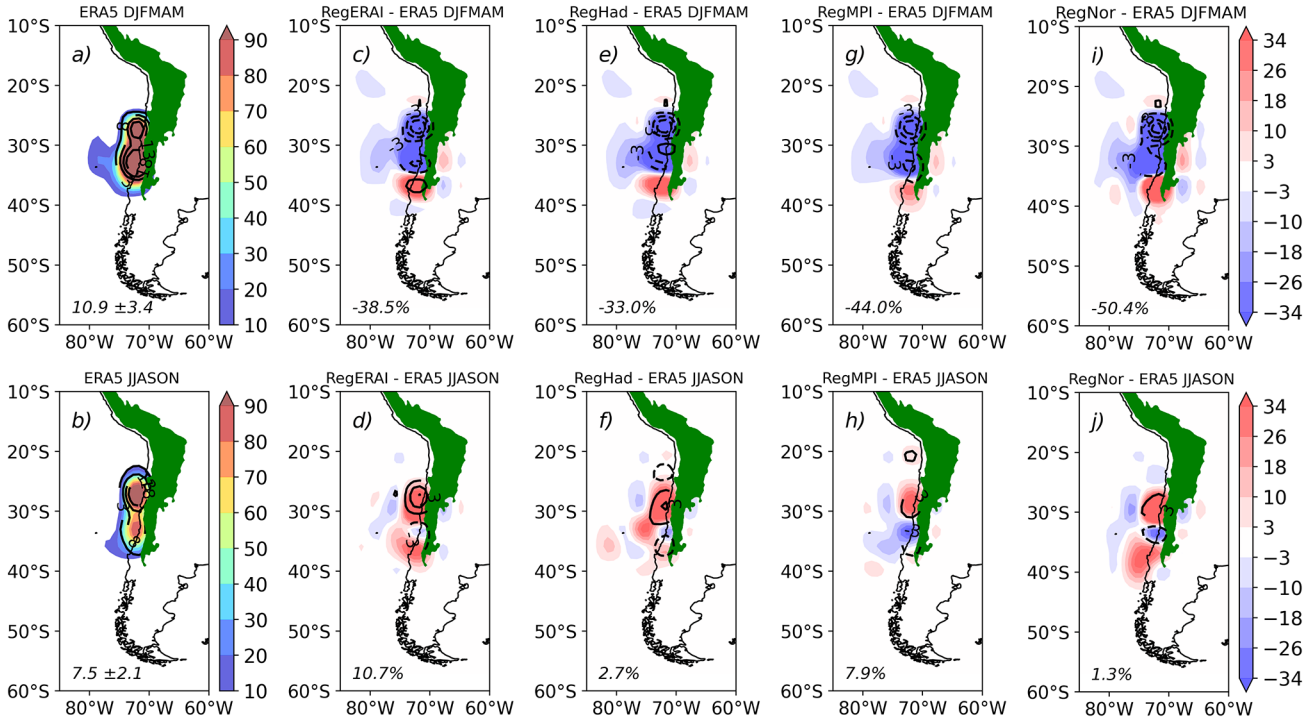

Fig. 3 (a-b) Seasonal climatology of CLs genesis (lines; interval of 5) and track (shaded) densities in ERA5 and the simulated difference (bias) with respect to ERA5: (c-d) RegERAI, (e-f) RegHad, (g-h) RegMPI and (i-j) RegNor. The top (bottom) panels refer to summer (winter); topography above 1500 m is masked in green. The units are cyclones per area (km²) x 10^6 per year. In the bottom of each panel are shown the seasonal mean and standard deviation of CLs for ERA5 and their relative biases (%) in simulations

both winter and summer. The adiabatic heating around 30°-40°S over the Andes and west coast can be inferred through the higher temperatures than the neighborhood at 925 hPa (Fig. 5a).

The composites in Figs. 4 and 5 are in agreement with those shown in Garreaud et al. (2002) for austral winter. By the time of CL formation (0 h), SPSH is intensified by a mid-tropospheric ridge, and a surface transient anticyclone develops to the east of the Andes. This anticyclone reinforces easterly winds towards the Cordillera, warming up and drying the Chilean central Valley (Rutllant and Garreaud 2004; Muñoz et al. 2020). 24 and 48 after genesis, the SPSH tends to weaken while the temperature and winds over the continent decrease.

In general the four simulations tend to underestimate (with respect to ERA5) the SLP field southwards of 40°S over the South Pacific and to overestimate it over the South Atlantic (as shown in Fig. 4b-e). The simulations, thus, tend to produce weaker anticyclonic circulation between the South Pacific and SA (Fig. 4b-e), especially RegMPI. Because of that, the simulations present lower temperatures over the southern tip of SA and higher temperatures over continental areas in the latitudinal band of 30°-40°S due to a stronger northerly flow east of the Andes (Fig. 5b-e). On the other hand, at this same latitude band, in the western side of the Andes there is a cold bias, which might indicate a less efficient adiabatic heating due to the weaker circulation of the near-surface anticyclone.

4.2 Cyclones affecting the coast (CACs)

Here, we discuss the cyclones classified as CAC, which will be divided in two classes: "not crossing the Andes" (that disappears near the coast) and "crossing the Andes".

4.2.1 Track and displacement

a) Not crossing the Andes

The cyclones classified as not crossing the Andes represent ~ 76% of all CAC and are more frequent during winter (~ 32 systems) compared to summer (~ 19 systems; Fig. 6a-b). RegHad and RegMPI tend to reproduce better the ERA5 frequency of the systems in summer (Fig. 6e,g). On the other hand, in winter all the simulations underestimate the number of systems by ~ 22% on average. In terms of track density, there is an underestimation of the signals in the offshore areas of the continent (over the South Pacific) in both seasons.

The underestimation of cyclones might be due to the differences in the simulated strength of the upper-level jets.

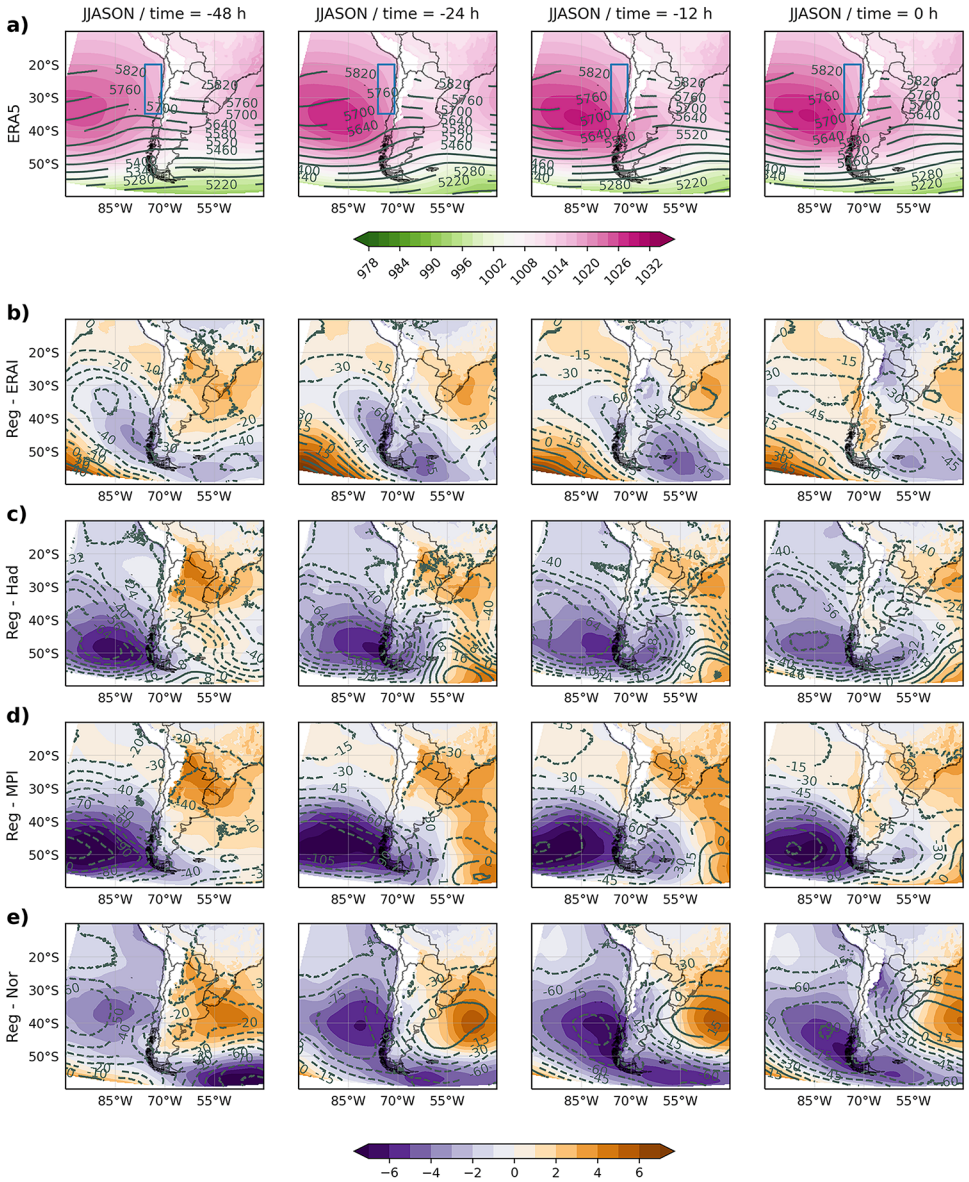

Fig. 4 Climatological evolution of the synoptic environment (from 48 h previous until genesis) of CLs in winter. a) SLP (shaded; hPa) and geopotential height at 500 hPa (m; lines) in ERA5 and b-e) the bias of the simulations regarding ERA5 (model "minus" ERA5; dashed lines indicate negative values). The blue rectangle in a) indicates the region of CLs genesis

In fact, all simulated upper-level jets tend to be weaker (by ~ 5–10 m s^{-1}) to the north of 30°S (figures not shown). This could affect the movement of cyclones over western South Pacific towards the selected domain. Moreover, jet streams located to the north of 30°S are important for cutoff low formation (Garreaud and Fuenzalida 2007) which could generate CACs' development and intensification over the eastern South Pacific (Campetella and Possia 2007). In contrast, there is an overestimation of cyclone track density along the west coast of SA and southern 50°S - possibly due to the fact that cyclones move faster - confirming, as mentioned above, the stronger simulated jet streams at higher latitudes. Note that Fig. 6 shows the first detected location (lines) inside the tracking domain of CACs not crossing Andes, which does not necessarily indicate the actual genesis site.

b) Crossing the Andes

The numbers of CACs that cross the Andes are quite similar for both seasons, as also their track density (Fig. 7a-b). Two higher frequency centers, one over the South Pacific and the other over the South Atlantic, indicate that systems crossing the Andes might regenerate near 45°S-60°W and/or be intensified by the Brazil-Malvinas currents confluence, which transfers baroclinicity to the atmosphere (Reboita et al. 2012). Simulations tend to overestimate the number of

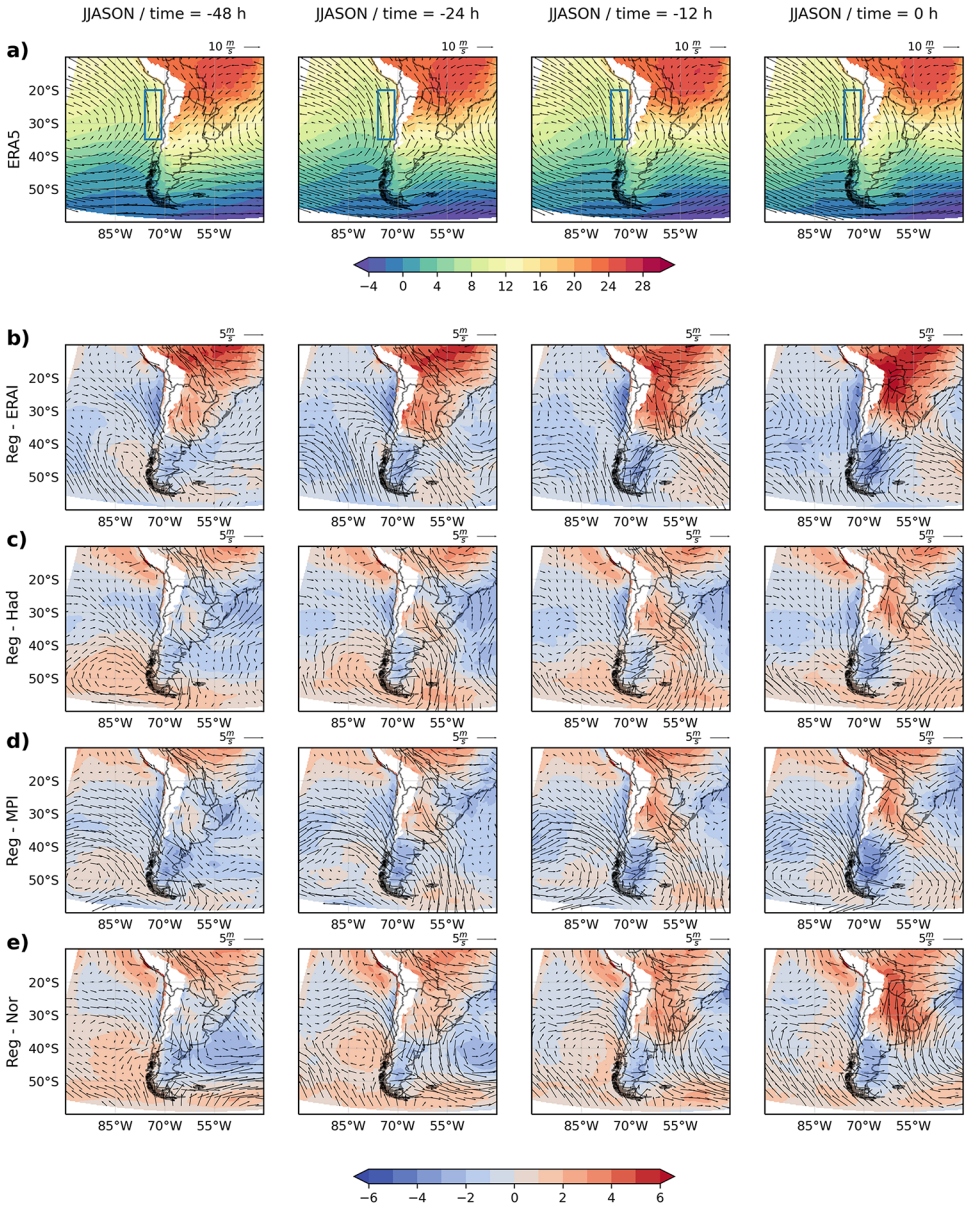

Fig. 5 Climatological evolution of the synoptic environment (from 48 h previous until genesis) of CLs in winter. a) Winds (vectors; m s^{-1}) and temperature (shaded; °C) at 925 hPa in ERA5 and b-e) the bias of the simulations regarding ERA5 (model "minus" ERA5). The blue rectangle in a) indicates the region of CLs genesis

systems in both seasons, especially in winter. This overestimation could be explained by the combination of simulated stronger upper-level jets and lower SLP over the region, especially southwards of 40°S (figure not shown). In both seasons, RegERAI and RegNor are in better agreement with ERA5 (Fig. 7c-d and i-j), due to their better representation of the SLP field over the South Pacific (figure not shown). RegMPI and RegHad basically simulate a double of systems during winter with respect to ERA5 (Fig. 7f, h).

4.2.2 Time evolution

Figures 8, 9 and 10 show the synoptic evolution of different atmospheric variables for CAC not crossing the Andes, from 24 h prior (-24) to after (+24) genesis, and the bias of the simulations with respect to ERA5. Considering ERA5 (Fig. 8a), a mid-level low-amplitude trough is centered in ~88°W 24 h previous to the cyclogenesis accompanied by relatively lower pressures underneath over the South Pacific (around 40°-50°S), while at 200 hPa the upper-level jet is zonally oriented between 30°-40°S, from the South Pacific

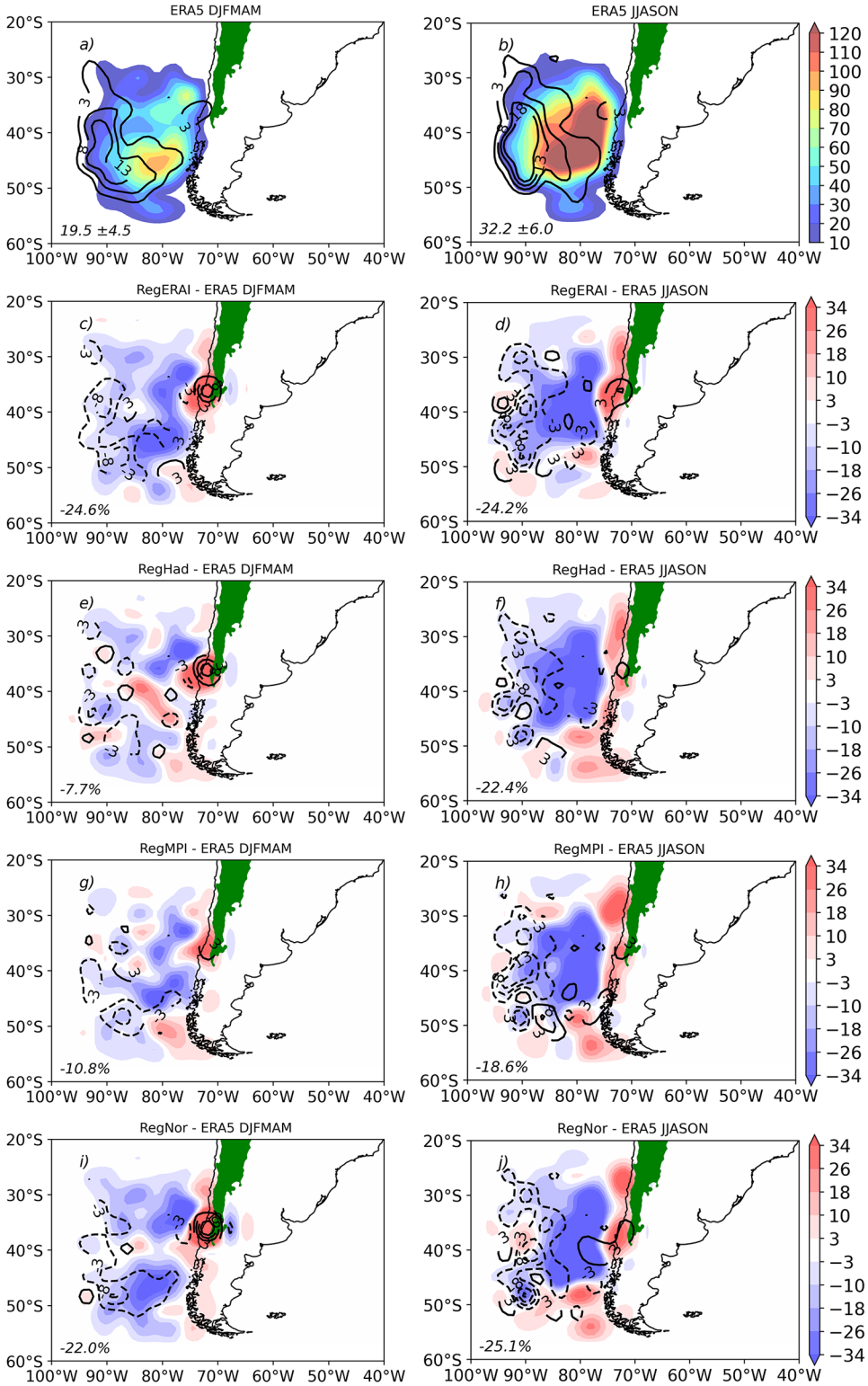

Fig. 6 Seasonal climatology of CACs that do not cross the Andes in their first detection (lines; interval of 5) and track (shaded) densities inside the domain in (a-b) ERA5 and the bias of the simulations regarding ERA5: (c-d) RegERAI, (e-f) RegHad, (g-h) RegMPI and (i-j) RegNor. The left (right) panels refer to summer (winter); topography above 1500 m is masked in green. The units are cyclones per area (km²) x 10^6 per year. In the bottom of each panel are shown the seasonal mean and standard deviation of first detection of CACs that do not cross the Andes for ERA5 and their relative biases (%) in simulations

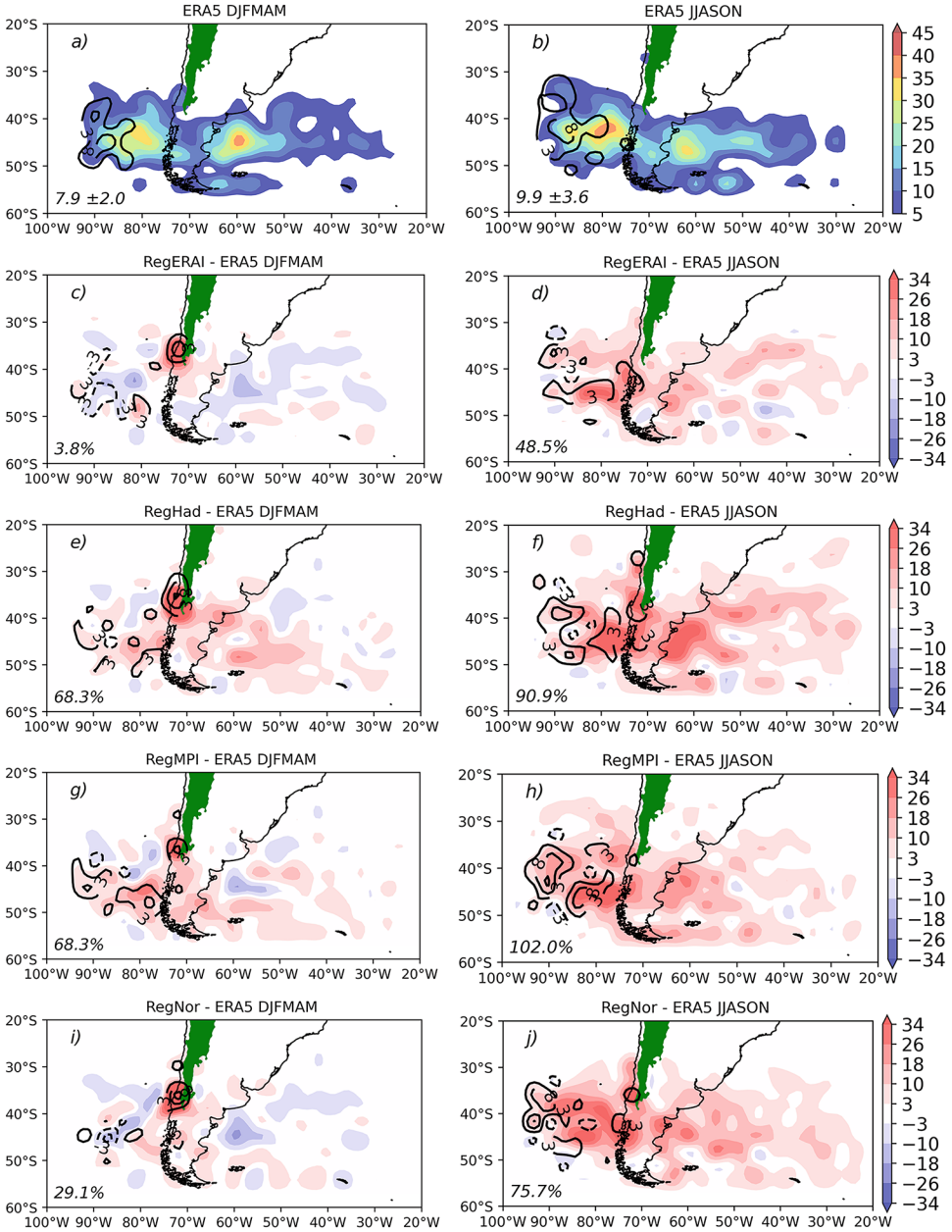

Fig. 7 Seasonal climatology of CACs that cross the Andes in their first detection inside the domain (lines; interval of 5) and track (shaded) densities in (a-b) ERA5 and the bias of the simulations regarding ERA5: (c-d) RegERAI, (e-f) RegHad, (g-h) RegMPI and (i-j) RegNor. The left (right) panels refer to summer (winter); topography above 1500 m is masked in green. The units are cyclones per area (km²) x 10^6 per year. In the bottom of each panel are shown the seasonal mean and standard deviation of first detection of CACs that cross the Andes for ERA5 and their relative biases (%) in simulations

to the South Atlantic (Fig. 10a). At the same time, the southerly winds in the eastern side of the SPSH contribute to northward advection of cold and dry air along the west coast of SA in lower latitudes (Fig. 9a). However, large amounts of precipitation are found to the south of 30°S as a consequence of the cyclone approaching the continent, especially over land (Fig. 11a).

Although the simulations are able to reproduce qualitatively well the spatial pattern of the atmospheric fields shown by ERA5 at this time step, they tend, in general, to overestimate the SLP southern 40°S over the South Pacific, mainly RegERAI and RegNor (Fig. 8b-e). These pressure differences do not seem to significantly affect the wind intensity in the simulations (biases of up to ± 2 m s^{-1}; Fig. 9b-e) but they affect precipitation over land and ocean. As the simulations

adequately represent the low-level winds, the reason for the cold bias along the coast of Chile could be associated with cloud cover and precipitation. Indeed, in Fig. 11b-e there is an overestimation of accumulated precipitation over Chile (to the north of 40°S) and Argentina (to the south of 40°S) in all simulations, whereas underestimation occurs over the ocean and near the coast. Even knowing that precipitation biases must be analyzed carefully - since gridded data may contain errors and not accurately represent the reality of certain regions, or extreme events, especially the ones with few observations (Tozer et al. 2012) -, our intention is to provide a general view of the climatological signal of precipitation associated with CACs that do not cross the Andes. Simulations also capture well specific humidity fields, except northward of 30°S where a moist bias over the South Pacific and a dry one over the continent are noted (Fig. 9b-e). Moreover at 200 hPa the upper-level jet appears to be displaced southwards, as shown by the positive bias in the wind intensity mainly in RegHad and RegMPI (Fig. 10b-e).

On the cyclogenesis day (0) in ERA5, the most relevant differences in relation to the previous day are the amplification of the trough over the South Pacific, the slight curvature of the upper-level jet (Figs. 8a and 10a) and the amplified cyclonic circulation at lower levels (Fig. 9a). By now, it is noticeable that CACs have their genesis as a consequence of dynamic processes (mid-latitude baroclinic waves). This is in agreement with previous studies, such as Vera et al. (2002), Hoskins and Hodges (2005), and Reboita et al. (2012). The biases in the simulations follow the same pattern described in -24, except by the low-level winds showing that simulations produce weaker cyclones compared to ERA5 (approximately 15% weaker; Fig. 9).

The atmospheric fields 24 h after the cyclogenesis (+24) show a clear eastward displacement of the trough at mid-upper levels; at this time, the eastern sector of the trough reaches SA (Figs. 8 and 10). While the baroclinic wave crosses the Andes at mid-upper levels, cyclolysis occurs between the South Pacific and the Andes at the surface. Moreover it is also verified a weakening of the circulation at 925 hPa 48 h after genesis (figure not shown) on the eastern side of the SA, indicating no regeneration of the cyclones over the South Atlantic. Nevertheless, our study also shows that there are cyclones that weaken when they reach the continent and regenerate in the eastern side of SA after the upper-level baroclinic wave crosses the Andes (CACs crossing the Andes).

5 Summary and conclusions

This study assesses the performance of RegCM4 in simulating cyclones that impact the western coast of South America (SA). First, a background of what classes of cyclones affect the western SA was presented through two case studies, describing the evolution of synoptic fields accompanied by the impacts near the coast. These first analyses focused on extratropical cyclones (ECs) and Coastal Lows (CLs). The second step consisted in tracking the cyclones using an automatic algorithm based on relative vorticity. The algorithm was applied to the ERA5 reanalysis, which was our reference dataset for comparison and in four RegCM4 simulations forced by ERA-Interim and three GCMs for the period 1995–2005.

Cyclones were then classified into three classes: CLs and ECs affecting the coast (CAC) splitted into the ones that do not cross the Andes and the ones that cross the Andes. The assessment was based on genesis and track densities and the synoptic evolution of the cyclones. The results in ERA5 and in the respective simulations - named as RegERAI, RegHad, RegMPI and RegNor - showed that for:

Coastal Lows

- They are more frequent during austral summer than in winter. In summer there are two centers of genesis around 30°S, whereas in the winter CLs are more meridionally extended and their offshore movement is smaller than in summer;
- In summer, simulations underestimate genesis and track density equatorwards of 35°S, whereas polewards of this latitude there is an overestimation. RegNor underestimates by 50% the CL genesis, which might be due to the coarser resolution and to a weaker simulated SPSH in the driving GCM;
- In winter, simulations overestimate genesis and track densities of CLs, especially RegERAI (~11% more systems). One explanation might be due to the more intense and much closer to the continent SPSH in the simulation;
- During the CL evolution, the four simulations produce a weaker anticyclonic circulation between the South Pacific and SA. With a weaker flow crossing the Andes at latitudes near 45°S, lower temperatures are simulated over the southern tip of SA and higher temperatures over continental areas in the latitudinal band of 30°-40°S.

Cyclones crossing the Andes

- The number of systems and their track density are quite similar for winter and summer;
- The simulations overestimate the number of systems in both seasons, especially during winter. This could be explained by the combination of the stronger upper-level jets and weaker SLP in the simulations, especially southwards of 40°S;

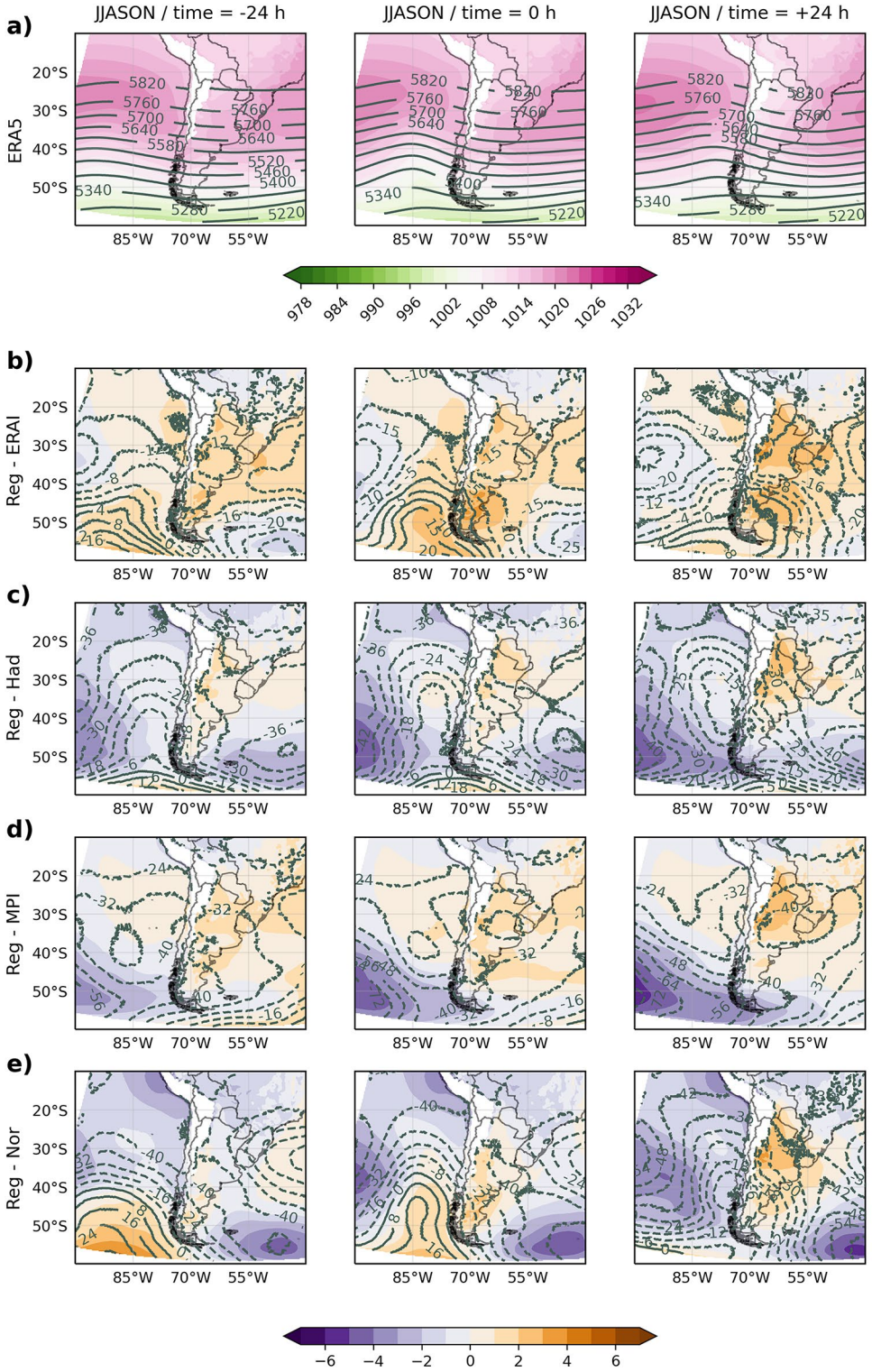

Fig. 8 Climatological evolution of the synoptic environment (from 24 h previous until 24 h after genesis) of CAC not crossing the Andes in winter. a) SLP (shaded; hPa) and geopotential height at 500 hPa (lines; m) in ERA5 and b-e) the bias of the simulations regarding ERA5 (model "minus" ERA5; dashed lines indicate negative values)

- The simulations that show better performance are RegE-RAI and RegNor.

Cyclones not crossing the Andes

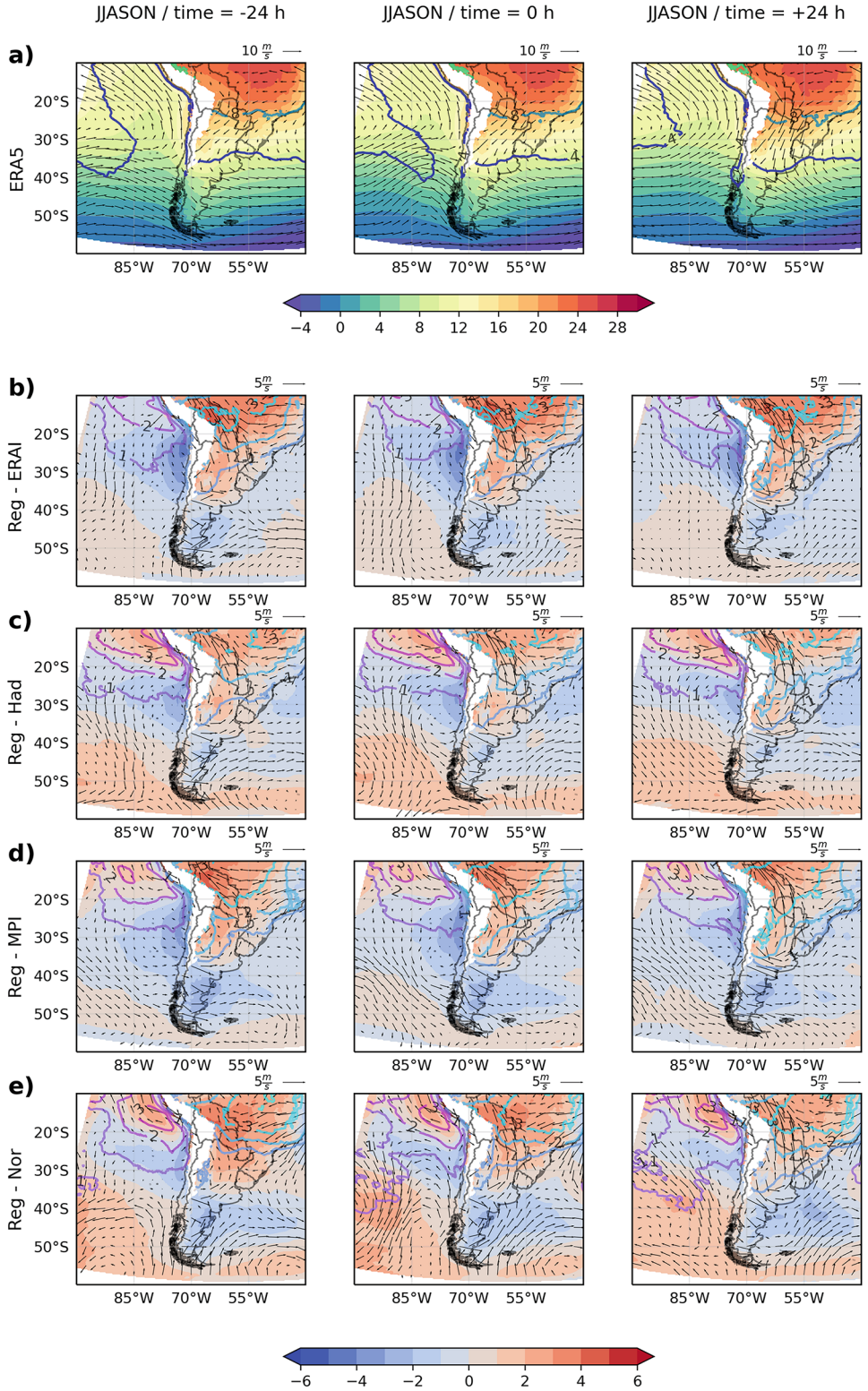

Fig. 9 Climatological evolution of the synoptic environment (from 24 h previous until 24 h after genesis) of CAC not crossing the Andes in winter. a) Winds (vectors; m s^{-1}) and temperature (shaded; °C) at 925 hPa and specific humidity (continuous lines; intervals of 4, 8, 12 g kg^{-1}) at 850 hPa in ERA5 and b-e) the bias of the simulations regarding ERA5 (model "minus" ERA5; lines intervals from − 4 to 4 at each 1 g kg^{-1})

- They represent ~ 76% of all CAC and are more frequent during winter than summer;

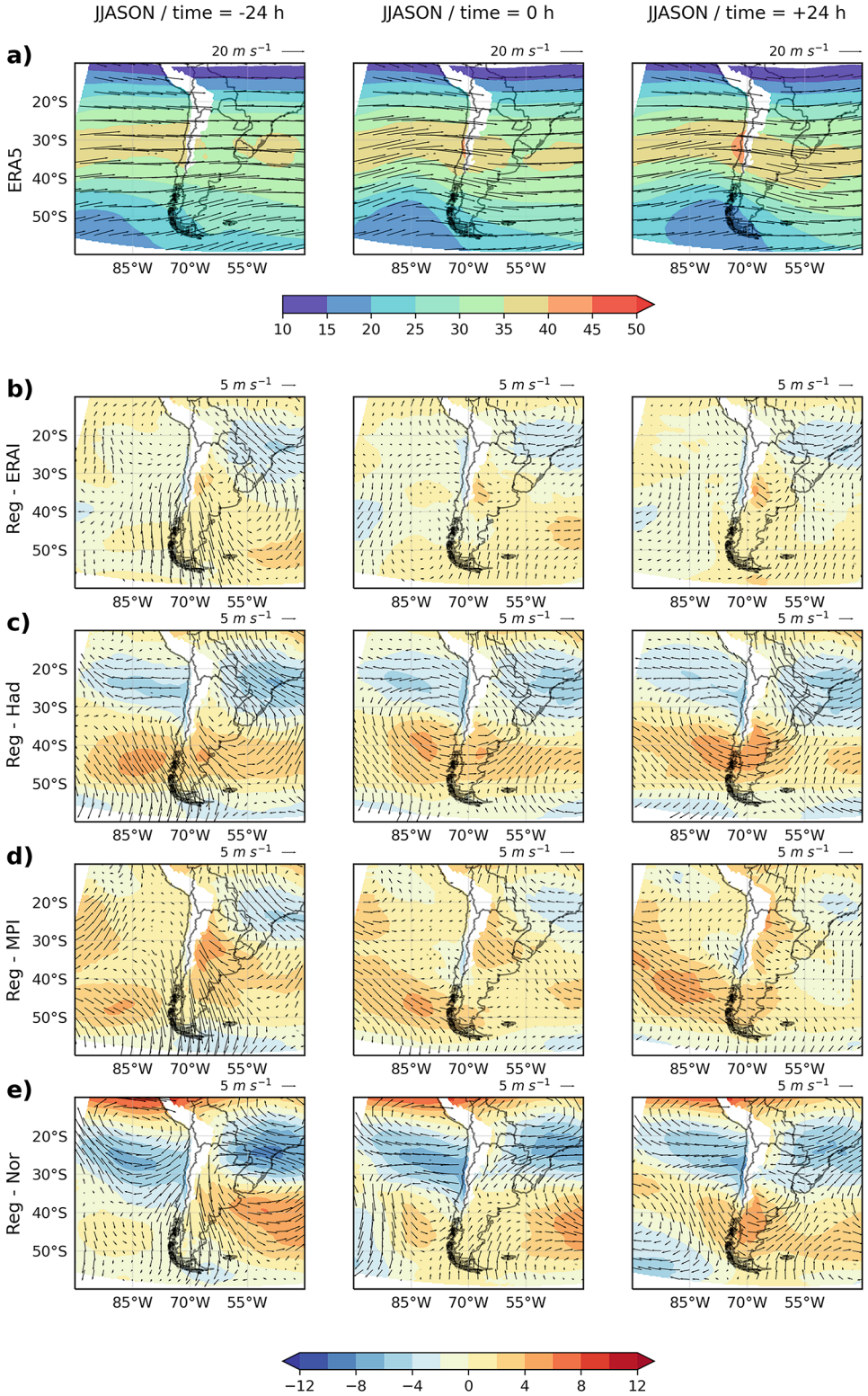

Fig. 10 Climatological evolution of the synoptic environment (from 24 h previous until 24 h after genesis) of CAC not crossing the Andes in winter. a) Winds vectors and intensity (m s^{-1}) at 200 hPa in ERA5 and b-e) the bias of the simulations regarding ERA5 (model "minus" ERA5)

- RegHad has small bias of the number of systems that are first detected inside the domain during summer, whereas all simulations underestimate the number of systems by ~ 22% in winter;

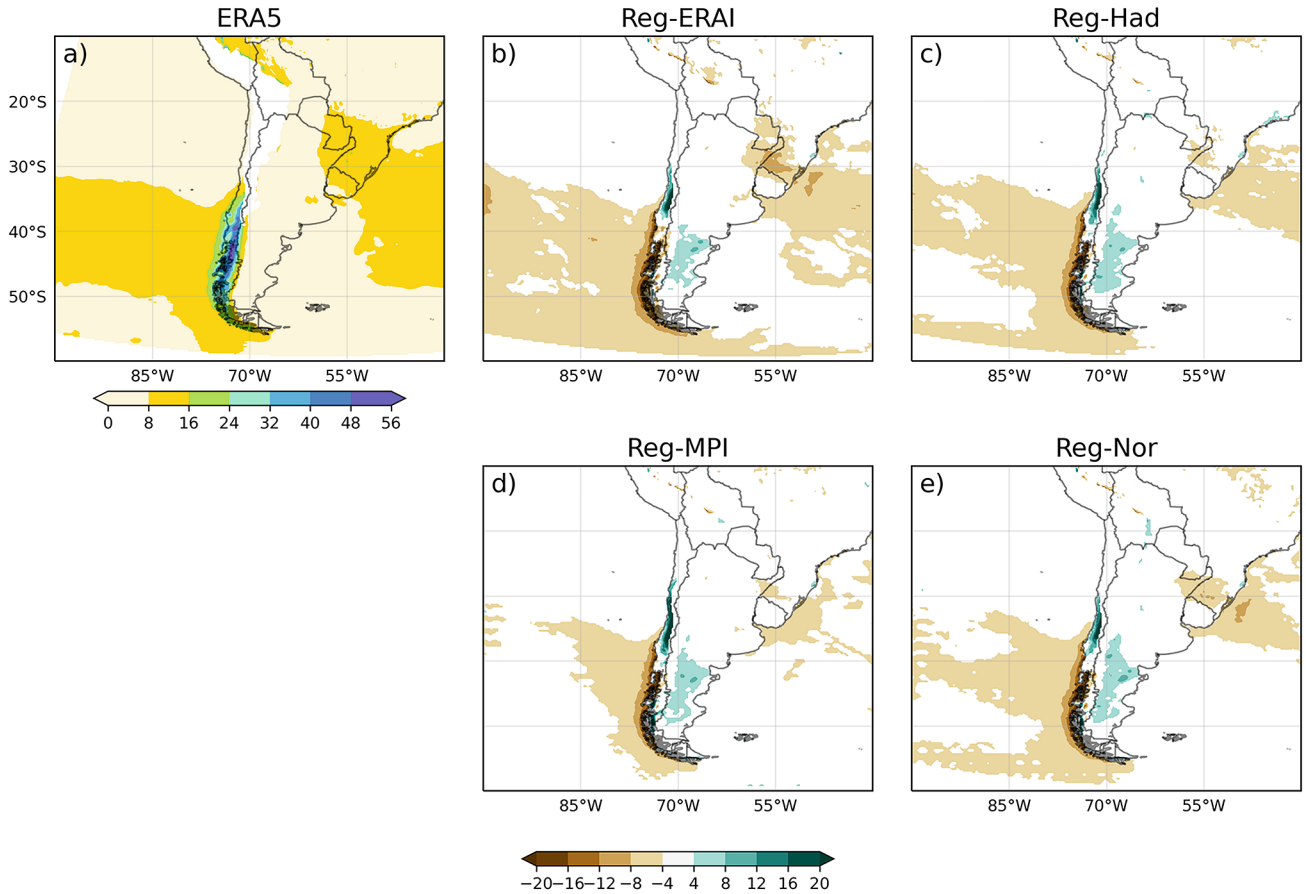

Fig. 11 Climatological accumulated precipitation (mm) from 24 h previous until 24 h after the first detection of CAC not crossing the Andes in winter in a) ERA5 and b-e) the bias of the simulations regarding ERA5 (model "minus" ERA5)

- There is an underestimation in the frequency of cyclones by the simulations in the offshore areas of the domain (over the South Pacific) that might be associated with the simulated strength of the upper-level jets, which in all simulations are weaker (by ~5–10 m s^{-1}) than in ERA5 to the north of 30°S. In contrast, the overestimation along the west coast of SA might be related with a faster movement of the simulated cyclones and the stronger jet streams at higher latitudes;
- RegERAI and RegNor have better performances to represent the synoptic evolution of these systems.

This study contributes to the knowledge of cyclones that affect the western coast of SA by describing their synoptic characteristics, impacts, seasonality and, more importantly, the ability of RegCM4 in simulating them in a systematic way. Overall, the RegCM4 is able to represent the characteristics of both ECs and CLs, with better representation when forced by specific GCMs. Further studies on how these results rely on GCMs are important.

This is a first assessment that provides initial knowledge for further studies on how climate change impacts cyclones over the region. Moreover, understanding these systems' evolution and monitoring them is very important for planning and mitigation strategies in order to avoid negative impacts along the western coast of SA and over Chile (such as abrupt air temperature changes over the continent, enhancement of air pollutants and high accumulated precipitation).

Acknowledgements This collaborative research is the product of a capacity building activity organized by CORDEX-WCRP to promote collaborative activities and networking and to enhance the capacity to document scientific research in Central America and the Caribbean, and South America with focus on specific regional climate phenomena (http://www.cima.fcen.uba.ar/cordex-2020/). The authors thank all the international centres that provided the datasets for this study and for the anonymous reviewers that made suggestions and comments to improve the quality of the paper. N.M.C, M.S.R, L.F.G., E.M.J. and R.P.R. thank CAPES, CNPq and PETROBRAS for the financial support. M.R. has been supported in this work by OGS and CINECA under HPC-TRES award number 2015-07 and by the project FAIRSEA (Fisheries in the Adriatic Region - a Shared Ecosystem. Approach) funded by the 2014 - 2020 Interreg V-A Italy - Croatia

CBC Programme (Standard project ID 10046951). M.L.Z. has been supported by the Chilean ANID Doctoral grant 21192178. L.F.T.R. has received funding support from FONDECYT through grant 1201742.

Author contributions All authors contributed to the study conception and design. Material preparation and data collection were performed by Natália Machado Crespo, Luiz Felippe Gozzo, Eduardo Marcos de Jesus, Miguel Ángel Lagos Zúñiga, José Abraham Torres Alavez and Limbert Fernando Torrez Rodriguez. The analyses were performed by Natália Machado Crespo, Michelle Simões Reboita and Luiz Felippe Gozzo. The first draft of the manuscript was written by Natália Machado Crespo, Michelle Simões Reboita, Luiz Felippe Gozzo, Miguel Ángel Lagos Zúñiga, Limbert Fernando Torrez Rodriguez and Marco Reale and all authors commented on previous versions of the manuscript. Rosmeri Porfirio da Rocha revised the manuscript. All authors read and approved the final manuscript.

Declarations.

Funding Not applicable.

Data Availability Not applicable.

Code Availability Not applicable.

Declarations

Conflicts of interest/Competing interests The authors declare that there are no conflicts of interest.

References

Aceituno P, Boisier JP, Garreaud R, Rondanelli R, Rutllant JA (2021) Climate and weather in Chile. In Water resources of Chile. Springer Cham, pp 7–29

Andrelina B, Reboita MS (2021) Climatologia do Índice do Potencial de Gênese de Ciclones Tropicais nos Oceanos Adjacentes à América do Sul. Anuário do Instituto de Geociências 44:39515. https://doi.org/10.11137/1982-3908_2021_44_39515

Barahona C (2013) Precipitaciones asociadas a Bajas Segregadas en la zona central de Chile, entre los años 2003 y 2005. Report to obtain a professional title in Meteorology. Universidad de Valparaíso

Barrett BS, Garreaud R, Falvey M (2009) Effect of the Andes Cordillera on precipitation from a midlatitude cold front. Mon Weather Rev 137(9):3092–3109

Belmonte Rivas M, Stoffelen A (2019) Characterizing ERA-Interim and ERA5 surface wind biases using ASCAT. Ocean Sci 15:831–852. https://doi.org/10.5194/os-15-831-2019

Bentsen M, Bethke I, Debernard JB et al (2013) The Norwegian Earth System Model, NorESM1-M–Part 1: description and basic evaluation of the physical climate. Geosci Model Dev 6(3):687–720

Campetella C, Possia N (2007) Upper-level cut-off lows in southern South America. Meteorol Atmos Phys 96:181–191. https://doi.org/10.1007/s00703-006-0227-2

Collins WJ, Bellouin N, Doutriaux-Boucher M et al (2008) Evaluation of the HadGEM2 model. Met Office, Exeter, UK, p 48

Crespo NM, da Rocha RP, Sprenger M, Wernli H (2021) A potential vorticity perspective on cyclogenesis over centre-eastern South America. Int J Climatol 41:663–678. https://doi.org/10.1002/joc.6644

Dalagnol R, Gramcianinov CB, Crespo NM et al (2022) Extreme rainfall and its impacts in the Brazilian Minas Gerais state in January 2020: Can we blame climate change? Clim Resil Sustain 1:e15. https://doi.org/10.1002/cli2.15

de Jesus EM, da Rocha RP, Crespo NM, Reboita MS, Gozzo LF (2021) Multi-model climate projections of the main cyclogenesis hot-spots and associated winds over the eastern coast of South America. Clim Dyn 56:537–557. https://doi.org/10.1007/s00382-020-05490-1

Dee DP, Uppala SM, Simmons AJ et al (2011) The ERA-Interim reanalysis: Configuration and performance of the data assimilation system. Q J R Meteorol Soc 137(656):553–597

Dullaart JCM, Muis S, Bloemendaal N et al (2020) Advancing global storm surge modelling using the new ERA5 climate reanalysis. Clim Dyn 54:1007–1021. https://doi.org/10.1007/s00382-019-05044-0

Elguindi N, Grundstein A, Bernardes S et al (2014) Assessment of CMIP5 global model simulations and climate change projections for the 21st century using a modified Thornthwaite climate classification. Clim Change 122:523–538. https://doi.org/10.1007/s10584-013-1020-0

Espinoza JC, Garreaud R, Poveda G et al (2020) Hydroclimate of the Andes Part I: main climatic features. Front Earth Sci 8:64

Flaounas E, Kelemen FD, Wernli H et al (2018) Assessment of an ensemble of ocean–atmosphere coupled and uncoupled regional climate models to reproduce the climatology of Mediterranean cyclones. Clim Dyn 51(3):1023–1040

Fuenzalida HA, Sánchez R, Garreaud RD (2005) A climatology of cutoff lows in the Southern Hemisphere.Journal of Geophysical Research: Atmospheres, 110(D18)

Gallardo L, Olivares G, Langner J, Aarhus B (2002) Coastal lows and sulfur air pollution in Central Chile. Atmos Environ 36(23):3829–3841

Gan MA, Rao VB (1991) Surface cyclogenesis over South America. Mon Weather Rev 119:1293–1302

Garreaud R (1999) Cold air incursions over subtropical and tropical South America: A numerical case study. Mon Weather Rev 127(12):2823–2853

Garreaud RD (2009) The Andes climate and weather. Adv Geosci 22:3–11

Garreaud R, Fuenzalida HA (2007) The Influence of the Andes on Cutoff Lows: A Modeling Study. Mon Weather Rev 135(4):1596–1613. https://doi.org/10.1175/MWR3350.1

Garreaud R, Rutllant J, Fuenzalida H (2002) Coastal lows along the subtropical west coast of South America: Mean structure and evolution. Mon Weather Rev 130(1):75–88

Garreaud RD, Rutllant J (2003) Coastal lows along the subtropical west coast of South America: Numerical simulation of a typical case. Mon Weather Rev 131(5):891–908

Giorgetta MA, Jungclaus J, Reick CH et al (2013) Climate and carbon cycle changes from 1850 to 2100 in MPI-ESM simulations for the Coupled Model Intercomparison Project phase 5. J Adv Model Earth Syst 5(3):572–597

Giorgi F, Coppola E, Solmon F et al (2012) RegCM4: model description and preliminary tests over multiple CORDEX domains. Climate Res 52:7–29

Giorgi F, Coppola E, Jacob D et al (2022) The CORDEX-CORE EXP-I Initiative: Description and Highlight Results from the Initial Analysis. BAMS 103(2):E293–E310. https://doi.org/10.1175/BAMS-D-21-0119.1

Gómez-Contreras Á, Ávila NC, Rapanague MJ, Rojas RR (2021) Coastal lows climatology along the Chilean coast using ERA5 reanalysis (No. EGU21-5656). Copernicus Meetings

Hersbach H, Bell B, Berrisford P et al (2020) The ERA5 global reanalysis. Q J R Meteorol Soc 146(730):1999–2049

Holton JR, Hakim GJ (2013) An Introduction to Dynamic Meteorology, 5th edn. Elsevier Academic Press, New York. https://doi.org/10.1016/C2009-0-63394-8

Hoskins BJ, Hodges KI (2005) A new perspective on southern hemisphere storm tracks. J Clim 18:4108–4129
Lionello P, Trigo IF, Gil V et al (2016) Objective climatology of cyclones in the Mediterranean region: a consensus view among methods with different system identification and tracking criteria. Tellus A: Dynamic Meteorology and Oceanography 68(1):29391
Marrafon VH, Reboita MS, da Rocha RP, Crespo NM (2021) Extratropical Cyclones in the Southern Hemisphere: comparison among different Reanalyses. Rev Bras Climatol 28:48–73
Molina MO, Gutiérrez C, Sánchez E (2021) Comparison of ERA5 surface wind speed climatologies over Europe with observations from the HadISD dataset. Int J Climatol 41:4864–4878. https://doi.org/10.1002/joc.7103
Muñoz C, Schultz DM (2021) Cutoff Lows, Moisture Plumes, and Their Influence on Extreme-Precipitation Days in Central Chile. J Appl Meteorol Climatology 60(4):437–454
Muñoz RC, Armi L, Rutllant JA et al (2020) Raco Wind at the Exit of the Maipo Canyon in Central Chile: Climatology, Special Observations, and Possible Mechanisms. J Appl Meteorol Climatology 59(4):725–749
Neu U, Akperov MG, Bellenbaum N et al (2013) IMILAST: A community effort to intercompare extratropical cyclone detection and tracking algorithms. Bull Am Meteorol Soc 94(4):529–547
Palmen E, Newton CW (1969) Atmospheric Circulation System. Academic Press, New York
Pezza AB, Ambrizzi T (2003) Variability of Southern Hemisphere cyclone and anticyclone behavior: further analysis. J Clim 16:1075–1083
Pezza AB, Durrant T, Simmonds I, Smith I (2008) Southern hemisphere synoptic behavior in extreme phases of SAM, ENSO, sea ice extent, and southern Australia rainfall. J Clim 21:5566–5584
Pezza AB, Rashid HA, Simmonds I (2012) Climate links and recent extremes in antarctic sea ice, high-latitude cyclones, Southern Annular Mode and ENSO. Clim Dyn 38:57–73
Pezza AB, Simmonds I (2005) The first South Atlantic hurricane: Unprecedented blocking, low shear and climate change. Geophys Res Lett 32. doi:https://doi.org/10.1029/2005GL023390
Pinheiro HR, Hodges KI, Gan MA, Ferreira NJ (2017) A new perspective of the climatological features of upper-level cut-off lows in the Southern Hemisphere. Clim Dyn 48:541–559
Portmann R, Sprenger M, Wernli H (2021) The three-dimensional life cycles of potential vorticity cutoffs: a global and selected regional climatologies in ERA-Interim (1979–2018). Weather and Climate Dynamics 2(2):507–534
Rahn DA, Garreaud RD (2014) A synoptic climatology of the near-surface wind along the west coast of South America. Int J Climatol 34:780–792. https://doi.org/10.1002/joc.3724
Rasmussen KL, Houze RA Jr (2016) Convective initiation near the Andes in subtropical South America. Mon Weather Rev 144(6):2351–2374
Reale M, Liberato ML, Lionello P, Pinto JG, Salon S, Ulbrich S (2019) A global climatology of explosive cyclones using a multi-tracking approach. Tellus A: Dynamic Meteorology and Oceanography 71(1):1611340
Reale M, Cabos Narvaez WD, Cavicchia L et al (2021) Future projections of Mediterranean cyclone characteristics using the Med-CORDEX ensemble of coupled regional climate system models. Clim Dyn. https://doi.org/10.1007/s00382-021-06018-x
Reboita MS, Nieto R, Gimeno L, Da Rocha RP, Ambrizzi T, Garreaud R, Krüger LF (2010) Climatological features of cutoff low systems in the Southern Hemisphere.Journal of Geophysical Research: Atmospheres, 115(D17)
Reboita MS, da Rocha RP, Ambrizzi T (2012) Dynamic and climatological features of cyclonic developments over southwestern South Atlantic Ocean. In: Veress B, Szigethy J (eds) Horizons in Earth Science Research, vol 6. Nova Science Publishers, Hauppauge, NY, USA, pp 135–160
Reboita MS, da Rocha RP, Ambrizzi T, Gouveia CD (2015) Trend and teleconnection patterns in the climatology of extratropical cyclones over the Southern Hemisphere. Clim Dyn 45(7–8):1929–1944
Reboita MS, Veiga JAP (2017) Análise Sinótica e Energética de um VCAN que Causou Chuva no Deserto do Atacama em Março de 2015. Revista Brasileira de Meteorologia 32:123–139
Reboita MS, da Rocha RP, de Souza MR, Llopart M (2018) Extratropical cyclones over the southwestern South Atlantic Ocean: HadGEM2-ES and RegCM4 projections. Int J Climatol 38(6):2866–2879
Reboita MS, da Rocha RP, Oliveira DMD (2019) Key features and adverse weather of the named subtropical cyclones over the Southwestern South. Atl Ocean Atmos 10(1):6. https://doi.org/10.3390/atmos10010006
Reboita MS, Reale M, da Rocha RP et al (2020) Future changes in the wintertime cyclonic activity over the CORDEX-CORE southern hemisphere domains in a multi-model approach. Clim Dyn. https://doi.org/10.1007/s00382-020-05317-z
Reboita MS, Crespo NM, Torres JA et al (2021) Future changes in winter explosive cyclones over the Southern Hemisphere domains from the CORDEX-CORE ensemble. Clim Dyn. https://doi.org/10.1007/s00382-021-05867-w
Rozante JR, Moreira DS, Gonçalves LGG, Vila DA (2010) Combining TRMM and Surface Observations of Precipitation: Technique and Validation Over South America. Weather Forecast 25:885–894
Rutllant J (1981) Subsidencia forzada sobre ladera andina occidental y su relación con un episodio de contaminación atmosférica en Santiago. Tralka 2(57):76
Rutllant J, Garreaud R (1995) Meteorological air pollution potential for Santiago, Chile: towards an objective episode forecasting. Environ Monit Assess 34(3):223–244
Rutllant J, Garreaud R (2004) Episodes of strong flow down the western slope of the subtropical Andes. Mon Weather Rev 132(2):611–622
Saide PE, Carmichael GR, Spak SN, Gallardo L et al (2011) Forecasting urban PM10 and PM2. 5 pollution episodes in very stable nocturnal conditions and complex terrain using WRF–Chem CO tracer model. Atmos Environ 45(16):2769–2780
Scaff L, Rutllant JA, Rahn D et al (2017) Meteorological interpretation of orographic precipitation gradients along an Andes west slope basin at 30 S (Elqui Valley, Chile). J Hydrometeorol 18(3):713–727
Schultz DM, Bosart LF, Colle BA et al (2019) Extratropical cyclones: a century of research on meteorology's centerpiece. Meteorological Monogr 59:16–11
Seluchi ME (1995) Diagnóstico e pronóstico de situaciones sinópticas conducentes a desarrollos ciclónicos sobre el Este de Sudamérica, vol 34. Geofísica Internacional, México, pp 171–186
Silva BA, Reboita MS, Crespo NM, da Rocha RP, Dutra LMM (2022) Ciclones Subtropicais Guará e Lexi Parte I: Estrutura Térmica e Características Gerais. Revista Brasileira de Geografia Física 15(1):333–342. https://doi.org/10.26848/rbgf.v15.1.p333-342
Simmonds I, Keay K (2000) Mean Southern Hemisphere Extratropical Cyclone Behavior in the 40-Year NCEP–NCAR Reanalysis. J Clim 13:873–885
Taylor KE, Stouffer RJ, Meehl GA (2012) An overview of CMIP5 and the experiment design. Bull Am Meteorol Soc 93(4):485–498
Teichmann C, Jacob D, Remedio AR et al (2021) Assessing mean climate change signals in the global CORDEX-CORE ensemble. Climate Dynamics1–24
Tozer CR, Kiem AS, Verdon-Kidd DC (2012) On the uncertainties associated with using gridded rainfall data as a proxy for

observed. Hydrol Earth Syst Sci 16:1481–1499. DOI: https://doi.org/10.5194/hess-16-1481-2012

Ulbrich U, Leckebusch GC, Grieger J, Schuster M et al (2013) Are greenhouse gas signals of Northern Hemisphere winter extra-tropical cyclone activity dependent on the identification and tracking algorithm? Meteorol Z 22(1):61–68

Valenzuela RA, Garreaud RD (2019) Extreme daily rainfall in central-southern Chile and its relationship with low-level horizontal water vapor fluxes. J Hydrometeorol 20(9):1829–1850

Vera CS, Vigliarolo PK (2000) A diagnostic study of cold-air outbreaks over South America. Mon Wea Rev 128:3–24

Vera CS, Vigiarolo PK, Berbery EH (2002) Cold season synoptic scale waves over subtropical South America. Mon Weather Rev 130(3):684–699

Yanase W, Niino H, Hodges K, Kitabatake N (2014) Parameter spaces of environmental fields responsible for cyclone development from tropics to extratropics. J Clim 27(2):652–671. https://doi.org/10.1175/jcli-d-13-00153.1

Terms and Conditions

Springer Nature journal content, brought to you courtesy of Springer Nature Customer Service Center GmbH (“Springer Nature”).
Springer Nature supports a reasonable amount of sharing of research papers by authors, subscribers and authorised users (“Users”), for small-scale personal, non-commercial use provided that all copyright, trade and service marks and other proprietary notices are maintained. By accessing, sharing, receiving or otherwise using the Springer Nature journal content you agree to these terms of use (“Terms”). For these purposes, Springer Nature considers academic use (by researchers and students) to be non-commercial.
These Terms are supplementary and will apply in addition to any applicable website terms and conditions, a relevant site licence or a personal subscription. These Terms will prevail over any conflict or ambiguity with regards to the relevant terms, a site licence or a personal subscription (to the extent of the conflict or ambiguity only). For Creative Commons-licensed articles, the terms of the Creative Commons license used will apply.
We collect and use personal data to provide access to the Springer Nature journal content. We may also use these personal data internally within ResearchGate and Springer Nature and as agreed share it, in an anonymised way, for purposes of tracking, analysis and reporting. We will not otherwise disclose your personal data outside the ResearchGate or the Springer Nature group of companies unless we have your permission as detailed in the Privacy Policy.
While Users may use the Springer Nature journal content for small scale, personal non-commercial use, it is important to note that Users may not:

1. use such content for the purpose of providing other users with access on a regular or large scale basis or as a means to circumvent access control;
2. use such content where to do so would be considered a criminal or statutory offence in any jurisdiction, or gives rise to civil liability, or is otherwise unlawful;
3. falsely or misleadingly imply or suggest endorsement, approval , sponsorship, or association unless explicitly agreed to by Springer Nature in writing;
4. use bots or other automated methods to access the content or redirect messages
5. override any security feature or exclusionary protocol; or
6. share the content in order to create substitute for Springer Nature products or services or a systematic database of Springer Nature journal content.

In line with the restriction against commercial use, Springer Nature does not permit the creation of a product or service that creates revenue, royalties, rent or income from our content or its inclusion as part of a paid for service or for other commercial gain. Springer Nature journal content cannot be used for inter-library loans and librarians may not upload Springer Nature journal content on a large scale into their, or any other, institutional repository.
These terms of use are reviewed regularly and may be amended at any time. Springer Nature is not obligated to publish any information or content on this website and may remove it or features or functionality at our sole discretion, at any time with or without notice. Springer Nature may revoke this licence to you at any time and remove access to any copies of the Springer Nature journal content which have been saved.
To the fullest extent permitted by law, Springer Nature makes no warranties, representations or guarantees to Users, either express or implied with respect to the Springer nature journal content and all parties disclaim and waive any implied warranties or warranties imposed by law, including merchantability or fitness for any particular purpose.
Please note that these rights do not automatically extend to content, data or other material published by Springer Nature that may be licensed from third parties.
If you would like to use or distribute our Springer Nature journal content to a wider audience or on a regular basis or in any other manner not expressly permitted by these Terms, please contact Springer Nature at

onlineservice@springernature.com